J. Biochem. 131, 461–468 (2002)

Close Location of the First Loop to the Third Loop of the Mitochondrial ADP/ATP Carrier Deduced from Cross-Linking Catalyzed by Copper-*o*-Phenanthroline of the Solubilized Carrier with Triton X-100[1]

Eiji Majima,*,† Masashi Takeda,* Satomi Miki,* Yasuo Shinohara,* and Hiroshi Terada*,[2]

**Faculty of Pharmaceutical Sciences, University of Tokushima, Shomachi-1, Tokushima 770-8505; and †APRO Life Science Institute, Kurosaki, Naruto 772-0001*

Received November 24, 2001; accepted January 12, 2002

Effects of the cross-linking catalyst copper-*o*-phenanthroline [$Cu(OP)_2$] on the bovine heart mitochondrial ADP/ATP carrier solubilized with Triton X-100 were studied under various conditions. Without detergent treatment, $Cu(OP)_2$ specifically catalyzed the formation of intermolecular disulfide bridges in submitochondrial particles between two Cys^{56} residues in the first loop facing the matrix space of the dimeric carrier [Majima, E., Ikawa, K., Takeda, M., Hashimoto, M., Shinohara, Y., and Terada, H. (1995) *J. Biol. Chem.* 270, 29548–29554]. However, an intramolecular disulfide bridge between Cys^{56} and Cys^{256} in the third loop was formed in the solubilized carrier. Proteolytic digestion of the carrier with lysylendopeptidase showed that it first cleaves the Lys^{42}-Gln^{43} bond and then the Lys^{48}-Gln^{49} bond of the first loop in the membrane-bound carrier, but it cleaves both sites almost simultaneously in the solubilized carrier. These features were observed only with the *m*-state carrier; the c-state carrier was not subject to any cross-linking or proteolytic digestion. It is suggested that the protruding first loop is located close to the third loop, which could be exposed to a certain degree.

Key words: ADP/ATP carrier, copper-*o*-phenanthroline, cross linking, intramolecular disulfide bridge, mitochondria.

The ADP/ATP carrier (AAC) is a major transporter in the mitochondrial inner membrane mediating exchange transport of ADP and ATP. Inter-conversion of the carrier between the m-state and c-state conformations has been shown to be essential for its transport activity (*1*). In these conformations, the binding site for the transport substrates faces the matrix side and cytosolic side, respectively, and the transport inhibitors bongkrekic acid (BKA) and carboxyatractyloside (CATR) fix these respective states by their binding specifically to the adenine nucleotide binding site (*1, 2*). The 30-kDa bovine heart mitochondrial AAC contains three large hydrophilic loops, M1, M2, and M3, facing the matrix space, containing cysteine residues Cys^{56}, Cys^{159} and Cys^{256}, respectively. These are effective probe residues for monitoring the states of these three loops (*3–5*).

From the discrete reactivities of these cysteine residues with various SH-reagents such as *N*-ethylmaleimide (NEM) and eosin-5-maleimide (EMA), we found that the M1 loop protrudes into the matrix space, and the M2 and M3 loops intrude into the membrane region (*3, 4*). In addition, copper-*o*-phenanthroline [$Cu(OP)_2$] and various S-S cross-linkers specifically cause the formation of an intermolecular disulfide bridge between two Cys^{56} residues of the functional dimeric carriers in bovine heart submitochondrial particles (*5, 6*). Labeling with EMA and NEM, and disulfide bridge formation are only observed in the m-state carrier, not in the c-state carrier due to translocation of the extruding M1 loop into the membrane by conversion to the c-state conformation. Therefore, a large magnitude translocation of the M1 loop is thought to take place during the interconversion between the m- and c-state conformations (*5, 7*).

Triton X-100 has been widely used to solubilize the AAC bound tightly to the membrane. A preparation of Triton X-100-solubilized AAC has been referred to as a Triton-shell, and the carrier is thought to retain intact functional properties essentially similar to those of the membrane bound carrier, such as susceptibility to BKA, CATR and transport substrates (*8*). Hence the Triton-shell has been commonly used for reconstitution of the carrier incorporated into phospholipid bilayer membranes (*9*).

[1] This work was supported by Grants-in-Aid for Scientific Research [No. 07557164 & 08457609 (to H.T.)] and Scientific Research on Priority Areas of "Channel-Transporter Correlation" [No. 08268237 (to H.T.)] from the Ministry of Education, Science, Sports and Culture of Japan

[2] To whom correspondence should be addressed. Fax: +81-88-633-9511, E-mail: hterada@ph.tokushima-u.ac.jp

Abbreviations: AAC, the 30 kDa monomeric ADP/ATP carrier; $(AAC)_2$, the 60 kDa intermolecularly cross-linked ADP/ATP carrier; AAC′, the 28 kDa intramolecularly cross-linked ADP/ATP carrier; $Cu(OP)_2$, copper-*o*-phenanthroline; BKA, bongkrekic acid; CATR, carboxyatractyloside; NEM, *N*-ethylmaleimide; EMA, eosin-5-maleimide; SDS, sodium dodecyl sulfate; MOPS, 3-(*N*-morpholino)propanesulfonic acid; CBB, Coomassie Brilliant Blue R-250; PVDF, polyvinylidene difluoride; DTT, dithiothreitol; TLCK, *N*-tosyl-L-lysyl chloromethyl ketone.

In this study, we examined the location of the loops facing the matrix space in Triton-shells mainly by disulfide bridge formation catalyzed by $Cu(OP)_2$ under various conditions, because solubilization of the carrier with Triton X-100 was expected to affect the formation of inter-loop disulfide bridges between Cys^{56} residues (*5*). If a change is observed, this could be a clue to understanding the conformational states of the 3 loops facing the matrix space in relation to the transport activity of the carrier.

EXPERIMENTAL PROCEDURES

Reagents—EMA was purchased from Molecular Probes (Eugene). *o*-Phenanthroline, $CuSO_4$, and lysylendopeptidase were from Wako Pure Chemical Industries (Osaka). CATR was from Sigma (St. Louis), and hydroxylapatite and AG 1-X8 were from Bio-Rad (Richmond). NEM and Triton X-100 were from Nacalai Tesque (Kyoto). BKA was a gift from Prof. Duine (Delft University of Technology).

Preparations of Bovine Heart Submitochondrial Particles—Submitochondrial particles and CATR-preloaded particles were prepared from bovine heart mitochondria as described previously (*3*). The amounts of protein in the submitochondrial particles were determined with a BCA protein assay kit (Pierce, Rockford) in the presence of 1% SDS using bovine serum albumin as a standard.

Solubilization of Submitochondrial Particles with Triton X-100—Submitochondrial particles (8 mg of protein/ml) were solubilized with 2.4% Triton X-100 (3 mg Triton X-100/mg of protein) in a solution comprising 0.5 M NaCl, 0.04 mM EDTA, and 8 mM MOPS (pH 7.2) at 0°C for 10 min, and the solubilized samples were immediately analyzed for cross-linking. To study the binding of BKA to AAC, submitochondrial particles were preincubated with BKA at 10 nmol/mg of protein for 10 min at 0°C.

Cross-Linking of the ADP/ATP Carrier by $Cu(OP)_2$—A solution of 200 μM $Cu(OP)_2$ was prepared just before use by mixing 400 μM $CuSO_4$ with 800 μM *o*-phenanthroline in a molar ratio of 1:2. The $Cu(OP)_2$ concentration is shown in terms of the Cu^{2+} concentration. Submitochondrial particles (4 mg of protein/ml) or their solubilized preparations (4 mg of protein/ml) in medium consisting of 250 mM sucrose and 10 mM Tris-HCl buffer (pH 7.2) were incubated with 100 μM $Cu(OP)_2$ at 0°C for 10 min. The reaction was terminated by adding 5 mM EDTA and 5 mM NEM. Then the samples (10 μg of protein) were subjected to SDS-PAGE in 12% polyacrylamide gels under non-reducing conditions according to Laemmli (*10*) and the intensities of bands stained with Coomassie Brilliant Blue (CBB) were determined (*5*).

EMA-Labeling of the ADP/ATP Carrier—The preparation of submitochondrial particles (4 mg protein/ml) solubilized with Triton X-100 was incubated with 80 μM EMA at 0°C for the specified periods in the dark. Then the samples were subjected to SDS-PAGE in 12% polyacrylamide gels under reducing conditions and the fluorescence intensities of the protein bands labeled with EMA were determined (*3*).

Determination of Cross-Linking Sites—Submitochondrial particles (5 mg protein), which had been treated with BKA (10 nmol/mg of protein) for 10 min at 0°C, were solubilized with Triton X-100 (3 mg/mg of protein), and then treated with 100 μM $Cu(OP)_2$ at 0°C for 10 min. After termination of disulfide bond formation with 5 mM EDTA and alkylation of the free SH-groups with 5 mM NEM, fractions containing cross-linked AAC were prepared by chromatography on a hydroxylapatite column and by gel filtration chromatography, as reported previously (*5*), dried in a SpeedVac concentrator, and subjected to SDS-PAGE in 12% polyacrylamide gels. Then the protein bands were transferred electrophoretically to a polyvinylidene difluoride membrane (PVDF, Bio-Rad) in a semi-dry blotter (*5*) and stained with 0.1% Ponceau S. The cross-linked carrier band on the mem-brane was cut off, and the membrane pieces were soaked in acetonitrile. The protein disulfide bonds were reduced by incubation in a solution consisting of 6 M guanidine HCl, 2 mM EDTA, 1 mg DTT, and 0.5 M Tris-HCl (pH 8.5) at 37°C for 2 h, and the cysteine residues were carboxamidomethylated with 2.4 mg iodoacetamide by incubation for 30 min at 25°C in the dark. The membrane pieces were washed with 2% acetonitrile and incubated with 0.5% polyvinylpyrrolidone-40 in 100 mM acetic acid for 30 min at 37°C. After washing thoroughly with ultra-pure water, the protein on the membrane was digested with 2 μg lysylendopeptidase in 200 mM Tris-HCl (pH 8.0) containing 10% acetonitrile for 17 h at 37°C. The peptide fragments obtained were separated by reversed-phase HPLC on a TSK gel ODS-120T column (0.46 × 15 cm, Tosoh) in a linear gradient of 12–52% acetonitrile for 80 min in 0.05% trifluoroacetic acid at a flow rate of 1.0 ml/min. Elution was monitored at 210 nm. Separately, the carrier protein, without $Cu(OP)_2$ treatment, was subjected to SDS-PAGE, transferred to a PVDF membrane, carboxamidomethylated with iodoacetamide or labeled with NEM, and digested with lysylendopeptidase in a similar way to that described above.

Proteolytic Digestion of the Carrier—Submitochondrial particles (4 mg of protein/ml) pretreated with BKA or CATR were incubated with a solution of 0.5 M NaCl, 0.05 mM EDTA, and 50 mM Tris-HCl (pH 8.0) with or without treatment with 2.4% Triton X-100 for 10 min at 0°C, and then the proteins in the preparations were digested with lysylendopeptidase (3.3 μg/mg of protein) for 20 min at 30°C. Digestion was terminated with 0.5 mM TLCK and 2.5% SDS, and the protein samples (10 μg of protein) were subjected to SDS-PAGE.

N-Terminal Amino Acid Sequence Analysis—The N-terminal amino acid sequences were determined with a HP G1005A Protein Sequencing System (Hewlett-Packard, Palo Alto).

RESULTS

1. EMA-Labeling of the ADP/ATP Carrier Solubilized with Triton X-100—In order to understand the solubilization process by Triton X-100, we monitored the change in the turbidity of particle suspensions treated with various amounts of Triton X-100 for 10 min after its addition at pH 7.2 and 0°C. As shown in Fig. 1, the optical absorbance at 600 nm (A_{600}) gradually and consistently decreased with the increase in the amount of Triton X-100, suggesting that proteins in the particle membrane are smoothly incorporated into the Triton-phospholipid micelles. The A_{600} value became less than 0.1 at 3 mg of Triton X-100/mg of protein, and did not change with higher amounts of Triton X-100 due to the complete solubilization of the particles. It is note-

worthy that these solubilization conditions are usually used for the reconstitution of AAC in phospholipid vesicles (*9*).

Next, we examined the reactivity of the carrier in Triton-shells with EMA, which specifically labels Cys^{159} in loop M2 in membrane-bound AAC (*3*). EMA-labeling is an efficient tool with which to monitor the state of the carrier in Triton-shells. As shown in Fig. 2, the fluorescence intensity of the carrier labeled with EMA on SDS-PAGE increased with the increase in the incubation period. The labeling proceeded very quickly for the first 1 min and then increased gradually. The results of time-dependent EMA-labeling of the membrane bound carrier without Triton X-100 treatment showed that the initial rapid labeling is due to the labeling of Cys^{159}, and the following slow labeling is due to the labeling of both Cys^{56} and Cys^{256} (*3*).

When the mitochondria were solubilized with Triton X-100 after treatment with the transport inhibitor BKA, the rapid EMA-labeling was significantly suppressed, whereas the slow labeling was unchanged, showing that BKA inhibits the EMA-labeling of Cys^{159}, whereas it has no effects on the labelings of Cys^{56} and Cys^{256} (Fig. 2). No EMA-labeling was observed in the case of the c-state carrier fixed by CATR in the solubilizing preparation, as is observed for the membrane-bound carrier (data not shown). The same conformation-dependent EMA-labeling was observed when EMA-labeling was performed on the solubilized preparation to which BKA and CATR were added after solubilization. These results show that the carrier solubilized with Triton X-100 undergoes inter-conversion between the m-state and c-state conformation, as reported by Beyer and Nuscher (*8*). As BKA is known to bind to the transport substrate recognition/binding site in loop M2 (*4*), the carrier in Triton-shells was shown to retain the conformation available for substrate binding.

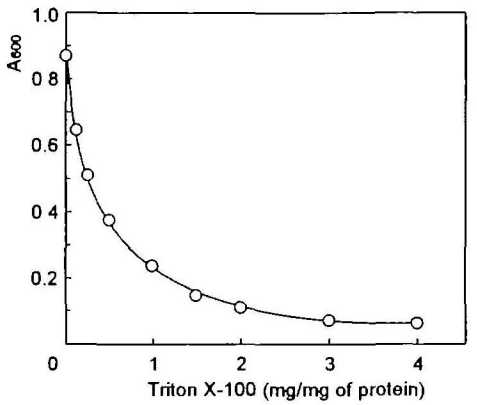

Fig. 1. **Solubilization of the ADP/ATP carrier with various amounts of Triton X-100.** Bovine heart submitochondrial particles (8 mg of protein/ml) were treated with various amounts of Triton X-100 in a solution of 0.5 M NaCl, 0.04 mM EDTA, and 8 mM MOPS (pH 7.2) at 0°C for 10 min. Then, the optical absorbance of the suspension was measured at 600 nm (A_{600}). Results are means (±SD) of three separate experiments.

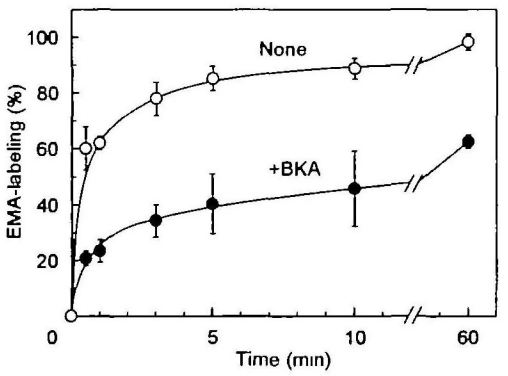

Fig. 2. **Time-course of EMA-labeling of the ADP/ATP carrier in Triton-shells.** Preparations of submitochondrial particles (4 mg protein/ml) solubilized in Triton X-100 (3 mg/mg of protein) in the presence or absence of BKA (10 nmol/mg of protein) were incubated with 80 μM EMA at pH 7.2 and 0°C for various periods in the dark. After termination of labeling, samples (20 μg of protein) were subjected to SDS-PAGE in 12% polyacrylamide gels under reducing conditions, and the fluorescence intensities of the protein bands labeled with EMA were determined. Results are means (±SD) of three separate experiments.

2. Effects of CATR and BKA on Cross-Linking of the Solubilized Carrier—The cross-linking of cysteine residues catalyzed by $Cu(OP)_2$ is an efficient means for monitoring changes in the states of the loops facing the matrix space. Therefore, we examined the effects of BKA and CATR on the cross-linking of the carrier in the membrane and Triton-shells. In the membrane bound carrier, submitochondrial particles pretreated with BKA or CATR were incubated with 100 μM $Cu(OP)_2$, and protein samples were subjected to SDS-PAGE under non-reducing conditions. As shown in Fig. 3, a 60-kDa band was observed in addition to

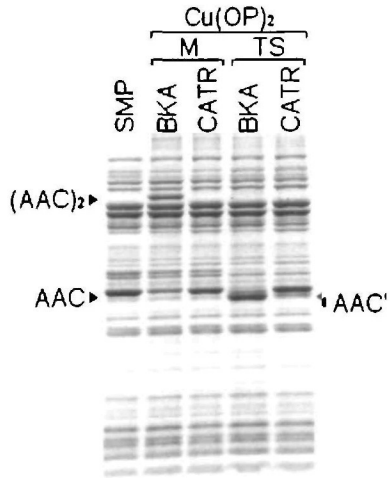

Fig. 3. **SDS-PAGE of mitochondrial proteins in the membrane and Triton-shells treated with $Cu(OP)_2$.** Submitochondrial particles (4 mg of protein/ml) suspended in medium consisting of 250 mM sucrose and 10 mM Tris-HCl (pH 7.2) treated with BKA (10 nmol/mg of protein) or CATR (4 nmol/mg of protein) were divided into two parts. One part was incubated with Triton X-100 (3 mg/mg of protein) for 10 min, and the other part was not. Then the two samples were incubated with 100 μM $Cu(OP)_2$ at 0°C for 10 min. After termination of the oxidation reaction, samples (10 μg of protein) were subjected to SDS-PAGE in 12% polyacrylamide gels under non-reducing conditions and the protein bands were stained with CBB. M, mitochondrial proteins in the membrane; TS, mitochondrial proteins in Triton-shells; SMP, submitochondrial particle without treatment with $Cu(OP)_2$. AAC, the ADP/ATP carrier; $(AAC)_2$, carrier dimerized through an intermolecular disulfide bond; AAC', carrier subjected to intramolecular disulfide bond formation.

the 30-kDa AAC band when the carrier was fixed in the m-state by BKA. Consistent with our previous results (*5*), amino acid sequence analysis showed that the 60-kDa band was due to dimeric AAC, referred to as $(AAC)_2$, created by the formation of an intermolecular disulfide bridge between two Cys^{56} residues, indicating that the M1 loops in the functional dimeric carrier are exposed to the matrix space. In contrast, $Cu(OP)_2$ did not affect the intensity of the 30-kDa AAC band upon treatment with CATR, showing that no cross-linking took place with the carrier in the c-state, as we observed previously (*5*).

When BKA-treated submitochondrial particles were solubilized with Triton X-100 then incubated with 100 μM $Cu(OP)_2$, a new 28-kDa band was formed, and no formation of $(AAC)_2$ was observed. As the 28-kDa band was reversed to the 30-kDa AAC band by treatment with the SH-reducing reagents DTT and 2-mercaptoethanol, the 28-kDa band was concluded to arise due to the formation of an intramolecular disulfide bridge in the 30-kDa AAC catalyzed by $Cu(OP)_2$. Hereafter, we refer to the 28-kDa carrier as AAC′. However, formation of neither the inter- nor intra-cross linking of the carrier was observed with the CATR-pretreated solubilized carrier. These results show that all the cysteine residues in the c-state carrier in Triton-shells are located in positions inaccessible to $Cu(OP)_2$, as in the case of the membrane bound carrier, and that the location of loops of the m-state carrier in Triton-shells is different from that of the membrane bound carrier.

We next examined the time-course of the effect of $Cu(OP)_2$ on the oxidation of cysteine residues of the m-state carrier in submitochondrial particles. As shown in Fig. 4A, the intensity of the 30-kDa AAC band decreased and that of the 60-kDa $(AAC)_2$ band increased as the incubation period with $Cu(OP)_2$ increased. For the m-state carrier in Triton-shells, however, no 60-kDa $(AAC)_2$ band was observed, but a new 28-kDa AAC′ band appeared at as early as 1 min, and the amount of AAC′ increased with time at the expense of the amount of 30-kDa AAC (Fig. 4B).

3. Dependence of Intramolecular Disulfide Bridge Formation on the Amount of Triton X-100—Submitochondrial particles were treated with various amounts of Triton X-100, and the samples were incubated with 100 μM $Cu(OP)_2$. Changes in the formation of AAC′ as a function of the amount of Triton X-100 were determined from the intensity of the AAC′ band on SDS-PAGE. Without detergent treatment, the relative amounts of the 30-kDa AAC and 60-kDa $(AAC)_2$ were 40 and 50%, respectively. As shown in Fig. 5, AAC′ was instantly formed even when the particles were treated with a small amount of Triton X-100 (= 0.1 mg/mg of protein). With increasing amounts of detergent, the formation of AAC′ proceeded hyperbolically accompanied by a decrease in the amount of $(AAC)_2$ up to 3.7 mg detergent/mg of protein. The amount of AAC remained almost constant up to 1.25 mg Triton X-100/mg of protein, and then decreased slightly. It is noteworthy that the change in the amount of $(AAC)_2$ was similar to the solubilization of the particles with Triton X-100 (see Fig. 1), showing that the solubilized carrier does not form an intermolecular disulfide bridge. These results suggest that Triton X-100 causes a change in location of the M1 loop away from the counterpart M1 loop of the functional dimeric carrier in such a way that the M1 loop is not able to form an intermolecular disulfide bond, tends to come close to other loop(s) to form an intramolecular disulfide bridge.

4. Identification of the Cross-Linking Site of the Solubi-

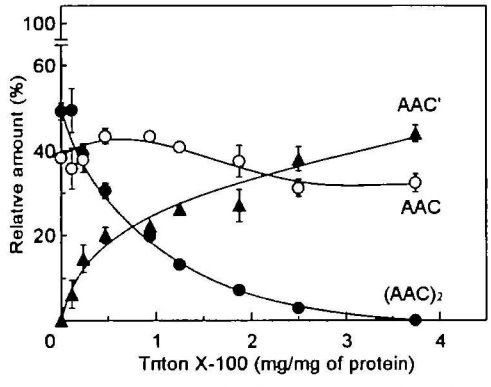

Fig. 5. **Change in the amounts of cross-linked products of the ADP/ATP carrier upon solubilization with various amounts of Triton X-100.** Submitochondrial particles (8 mg of protein/ml) were treated with various amounts of Triton X-100, and the samples (4 mg of protein/ml) were incubated with 100 μM $Cu(OP)_2$ for 10 min at pH 7.2 and 0°C. Changes in the amounts of AAC, AAC′, and $(AAC)_2$ as a function of the amount of Triton X-100 were determined from the band intensities on SDS-PAGE. The amounts relative to the total amount of carrier without $Cu(OP)_2$ treatment are shown. Values are means (±SD) of three separate experiments. Experimental conditions were as described for Fig. 4.

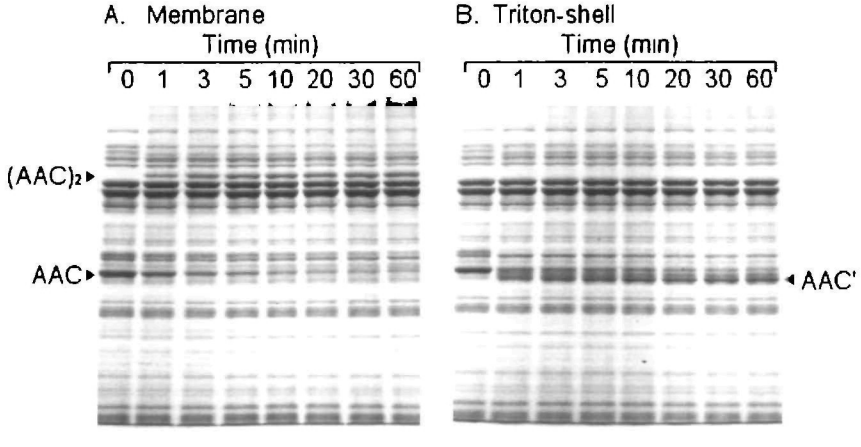

Fig. 4. **Cross-linking of the ADP/ATP carrier catalyzed by $Cu(OP)_2$ with or without Triton X-100 treatment.** Oxidation of the mitochondrial proteins was performed as described in the legend to Fig. 3, and the results of SDS-PAGE stained with CBB under non-reducing conditions in 12% polyacrylamide gels are shown. A: Submitochondrial particles (4 mg of protein/ml) were incubated with 10 nmol of BKA/mg of protein, and then treated with 100 μM $Cu(OP)_2$ for various periods at pH 7.2 and 0°C. B: BKA-treated particles (8 mg of protein/ml) were solubilized in Triton X-100 (3 mg/mg of protein), and the solubilized samples (4 mg/mg of protein) were incubated with 100 μM $Cu(OP)_2$ for various periods.

lized Carrier—We determined the cross-linking site(s) of the carrier catalyzed by $Cu(OP)_2$ in Triton-shells. Submitochondrial particles pretreated with BKA were solubilized with Triton X-100, and then incubated with 100 μM $Cu(OP)_2$. The oxidation reaction was terminated with EDTA and the unreacted free SH-groups were alkylated with NEM. The protein samples in the flow-through fractions from a hydroxylapatite column were solubilized, denatured with guanidine HCl containing NEM, and subjected to gel filtration chromatography. The fractions containing AAC and AAC′ were subjected to SDS-PAGE to separate AAC′ from AAC, and these samples were transferred to a PVDF membrane. The AAC′ on the membrane was treated with DTT to reduce the disulfide bond(s) and the reduced cysteine residues were carboxamidomethylated with iodoacetamide. By these treatments, the cysteine residues in the disulfide bridge(s) of the AAC′ were reduced and carboxamidomethylated, whereas cysteine residues that had not been oxidized were not carboxamidomethylated but alkylated with NEM. This modified AAC′ is referred to as RC-AAC′.

The solubilized carrier without $Cu(OP)_2$ treatment was used as a reference. The reference sample was treated with either NEM or iodoacetamide. By these treatments, all the cysteine residues were alkylated with NEM or carboxamidomethylated with iodoacetamide, and they are referred to as RNEM and RCAM, respectively. These reference preparations were digested with lysylendopeptidase, and the peptide fragments thus obtained were separated by reversed-phase HPLC on an ODS-120T column. Of the elution peaks, we identified those due to peptide fragments derived from both RNEM and RCAM, in which all 4 cysteine residues in the carrier were alkylated with NEM and caboxyamidemethylated with iodoacetamide, respectively (*3*). These peaks consisted of the peptide fragments Gln^{49}-Lys^{62}, Gln^{107}-Lys^{146}, Gly^{147}-Lys^{162}, and Gly^{245}-Lys^{259}, containing Cys^{56}, Cys^{128}, Cys^{159}, and Cys^{256}, respectively. These peptides derived from RNEM are referred to as N56, N128, N159, and N256, and those from RCAM, as C56, C128, C159, and C256, respectively.

Similarly, we digested RC-AAC' with lysylendopeptidase, and performed reversed-phase HPLC on an ODS-120T column. As shown in Fig. 6, four peaks due to C56, C128, C159, C256, and two peaks due to N128 and N159 were observed in the chromatogram of peptide fragments of digested RC-AAC′. The peak heights of C56, C256, N128, and N159 were almost the same as those of the corresponding peptides derived from the reference RCAM and RNEM. The amounts of cysteine residues alkylated with NEM and carboxamidomethylated with iodoacetamide were determined from the peak heights relative to those of RCAM and RNEM, respectively. As shown in Fig. 7, almost all the Cys^{128} and Cys^{159} residues were labeled with NEM, but no alkylation of Cys^{56} and Cys^{256} of RC-AAC′ was observed. In contrast, all the Cys^{56} and Cys^{256}, but less than 15% of the Cys^{128} and Cys^{159} were carboxamidomethylated. The slight carboxamidomethylation of Cys^{128} and Cys^{159} may be due to incomplete alkylation with NEM treated after termination of the oxidation reaction with $Cu(OP)_2$ and/or to cross-linking of denatured molecules. These results clearly show that Cys^{56} and Cys^{256} are responsible for the intramolecular dis-

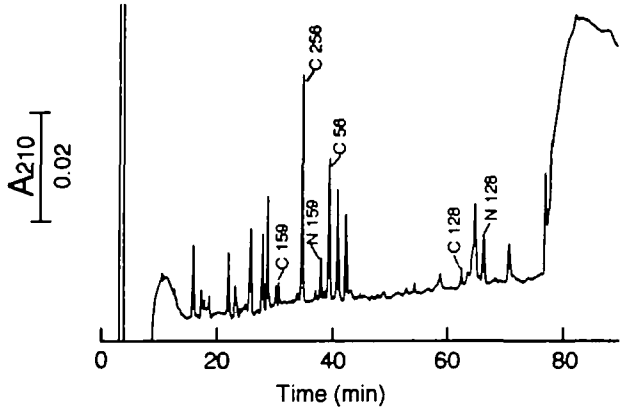

Fig. 6. **Analysis of the intramolecular disulfide bridge formation site of the ADP/ATP carrier in Triton-shells catalyzed by $Cu(OP)_2$.** Submitochondrial particles (5 mg protein) preteated with BKA were solubilized in Triton X-100 (3 mg/mg of protein), and then treated with 100 μM $Cu(OP)_2$ at 0°C for 10 min. After termination of the oxidation reaction, the solubilized samples were incubated with 5 mM NEM to alkylate free SH-groups. The flow-through fractions containing the carrier from a hydroxylapatite column were denatured with 6 M guanidine HCl and the free SH-groups of the carrier were alkylated with 1 mM NEM so that the free SH-groups were alkylated. Then, samples were subjected to gel filtration chromatography on a $G4000SW_{XL}$ column. Fractions containing the carrier were pooled and the carrier that had undergone intramolecular disulfide bridge formation (AAC′) was separated from the unreacted carrier by SDS-PAGE. The disulfide bond(s) of AAC′ was reduced with DTT in the presence of 6 M guanidine HCl, and then the reduced cysteine residues were carboxamidomethylated with iodoacetamide. Samples were digested with lysylendopeptidase and the peptide fragments obtained were separated by reversed-phase HPLC on a linear gradient of 12–52% acetonitrile for 80 min in 0.05% trifluoroacetic acid at a flow rate of 1.0 ml/min. Elution was monitored at 210 nm. C56, C128, C159, and C256 are peaks for peptide fragments containing carboxamidomethylated Cys^{56}, Cys^{128}, Cys^{159}, and Cys^{256}, respectively, and N128 and N159 are fragments containing Cys^{128} and Cys^{159} alkylated with NEM, respectively.

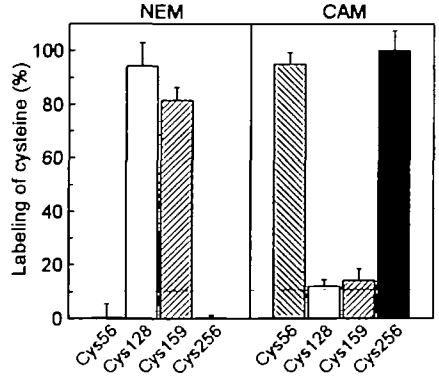

Fig. 7. **Amounts of alkylated and carboxamidomethylated cysteine residues in the ADP/ATP carrier in Triton-shells upon treatment with $Cu(OP)_2$.** Cross-linking was performed under the conditions described in the legend to Fig. 6. The amounts of NEM (NEM)- and carboxamidomethylated (CAM)-cysteine were determined from the peak heights of peptide fragments separated by reversed-phase HPLC, as shown typically in Fig. 6. Values are means (±SD) of three separate experiments, and shown relative to ADP/ATP carrier completely alkylated with NEM or carboxamidomethylated.

ulfide bridge formation in Triton-shells, suggesting that the M1 and M3 loops extrude close to the matrix space in Triton-shells.

5. Proteolytic Digestion of the Carrier—We examined the susceptibility of the membrane bound AAC and AAC in Triton-shells to the site-specific protease lysylendopeptidase. For this, submitochondrial particles preloaded with CATR and BKA were used. As seen in Fig. 8, in both preparations, lysylendopeptidase did not affect the c-state carrier, but cleaved the m-state carrier, giving two bands due to peptide fragments L-1 and L-2 derived from the 30-kDa AAC. We determined the N-terminal amino acid sequences of these fragments.

For this, submitochondrial particles pretreated with BKA were incubated with lysylendopeptidase, and subjected to SDS-PAGE in a 12% polyacrylamide gel. Peptide fragments in the gel were transferred to a PVDF membrane, and subjected to amino acid sequence analysis. From the results, the N-terminal amino acid sequences of L-1 and L-2 were determined to be Gln-Ile-Ser-Ala-Glu- and Gln-Tyr-X-Gly-Ile-, respectively. From the amino acid sequence of bovine heart AAC, L-1 and L-2 were peptides beginning from Gln^{43} and Gln^{49} of the carrier, respectively, indicating that lysylendopeptidase cleaves the bonds between Lys^{42}-Gln^{43} and Lys^{48}-Gln^{49} in loop M1. The cleavage of the carrier by lysylendopeptidase at the bond between Lys^{42}-Gln^{43} under similar conditions is consistent with the results of Marty *et al.* (*11*). However, they did not detect the second cleavage, possibly because the separation of the band L-1 from L-2 on SDS-PAGE was not insufficient due to the use of a high 20% concentration of polyacrylamide for the separation of short peptides by SDS-PAGE.

Next, we examined the time-course of proteolytic digestion of the m-state carriers in the membrane and Triton-shells. Submitochondrial particles preincubated with BKA were incubated with or without Triton X-100, and treated with lysylendopeptidase for various periods. After proteolysis, both samples were subjected to SDS-PAGE and the protein bands were stained with CBB. Then, the amounts of AAC, L-1 and L-2 were determined from the optical absorbance at 595 nm of the CBB extracted from the protein and peptide samples with 100 mM Tris-HCl buffer (pH 9.0). Figure 9 shows the results of the changes in the amounts of AAC, L-1, and L-2. In the case of the membrane-bound carrier, the amount of AAC decreased very rapidly, and almost disappeared after about 10 min. The amount of L-1 increased quickly and decreased after about 5 min, with the highest level being 65% attained at 5 min.

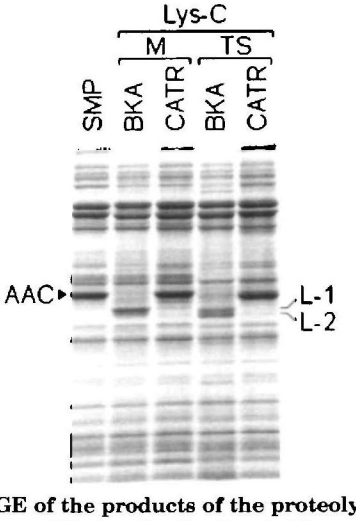

Fig. 8. **SDS-PAGE of the products of the proteolytic digestion with lysylendopeptidase of mitochondrial proteins in the membrane and Triton-shells.** Submitochondrial particles (4 mg of protein/ml) preloaded with BKA (10 nmol/mg of protein) or CATR (4 nmol/mg of protein), and their solubilized samples in Triton X-100 (3 mg/mg of protein) were incubated with lysylendopeptidase (3.3 μg/mg of protein) at 30°C for 20 min at pH 8.0. After termination of proteolysis with 0.5 mM TLCK and 2.5% SDS, samples (10 μg of protein) were subjected to SDS-PAGE in 12% polyacrylamide gels under reducing conditions. Protein bands were stained with CBB. Experimental conditions were as described for Fig. 3. Lys-C, mitochondrial proteins treated with lysylendopeptidase; M, proteins in the mitochondrial membrane; TS, proteins in Triton-shells; SMP, submitochondrial particle without lysylendopeptidase digestion; BKA and CATR, mitochondrial proteins treated with BKA and CATR, respectively; AAC, the 30 kDa ADP/ATP carrier remained undigested; L-1 and L-2, digested products of the ADP/ATP carrier.

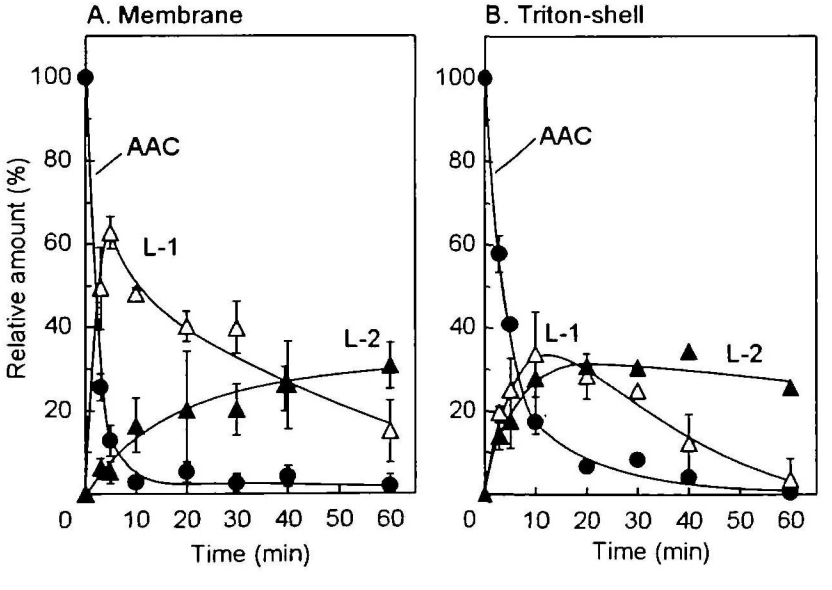

Fig. 9. **Time-course of the proteolytic digestion of the ADP/ATP carrier with lysylendopeptidase.** Submitochondrial particles pretreated with BKA were incubated with Triton X-100 (3 mg/mg of protein) for 10 min at pH 7.2 and 0°C. The particle suspensions without solubilization in Triton X-100, and those in Triton-shells were incubated with lysylendopeptidase for various periods at pH 8.0 and 30°C. Samples were subjected to SDS-PAGE and stained with CBB, as described in the legend to Fig. 8. Bands of AAC, L-1, and L-2 (see Fig. 8) were cut off, and the CBB was extracted with 100 mM Tris-HCl buffer (pH 9.0). The amount of CBB extracted was determined at 595 nm. A, membrane bound ADP/ATP carrier; B, carrier in Triton-shells. Values are means (±SD) of three separate experiments.

In contrast, the amount of L-2 increased gradually, reaching its highest level of 30% at about 60 min.

In contrast, a different digestion pattern was observed with the solubilized carrier preparation. The time-dependent decrease in the amount of AAC was slightly slower than that of the membrane-bound carrier. The formation of L-1 proceeded more slowly than in the case of the membrane-bound carrier, reaching its highest level of about 32% at about 10 min, a level lower than in the membrane-bound carrier. In addition, the rate of L-2 formation was slightly slower than that of L-1, but was much faster than in the case of the membrane bound carrier, and the highest amount of L-2 in the Triton-shells was similar to that of L-1. These results show that the bond between Lys^{48}-Gln^{49} of the carrier becomes more susceptible to proteolysis upon solubilization of the carrier. The fact that the combined total amounts of AAC, L-1, and L-2 are less than 100% at more than 10 min in both preparations suggests that AAC undergoes additional cleavage(s), although a band(s) representing the cleaved peptide fragment(s) was not detectable, possibly due to overlap with other protein bands on SDS-PAGE.

As L-2 appears after a decrease in the amount of L-1 in the case of the m-state carrier bound to the mitochondrial membrane, L-2 may be derived from the longer L-1 peptide. Possibly, the M1 loop extrudes from the membrane in such a way that the peptide segment containing the Lys^{42}-Gln^{43} bond is exposed, while the Lys^{48}-Gln^{49} bond is exposed to lesser extent. However, the carrier in Triton-shells undergoes proteolysis almost simultaneously at both sites, possibly because the M1 loop acquires more freedom of motion upon solubilization causing the second Lys^{48}-Gln^{49} bond to be more susceptible to protease attack.

DISCUSSION

Based on our recent results on the reactivities with SH-reagents of the three cysteine residues Cys^{56}, Cys^{159}, and Cys^{256}, which are located in three loops, M1, M2, and M3, facing the matrix space, respectively, we propose that a cooperative change in their locations is essentially important for the exhibition of transport activity of bovine heart mitochondrial AAC (*4, 7*). As a disulfide bridge between two Cys^{56} residues in a functional dimeric carrier is specifically formed in the m-state carrier, but not in the c-state carrier, by incubation with $Cu(OP)_2$, it is concluded that the first M1 loop extrudes into the matrix space in the m-state conformation and remains within the membrane in the c-state conformation. Hence, a large translocation of the M1 loop takes place upon interconversion between these two carrier conformational states (*5, 6*).

It is important to understand how the M1 loop achieves its translocation. Possibly, interactions of the M1 loop with other loops are associated with this translocation. We previously found that solubilization of the carrier with Triton X-100 results in the formation of an intramolecular disulfide bridge upon treatment with $Cu(OP)_2$, in contrast to the intermolecular disulfide bridge formed in the membrane bound carrier (*5*). This suggests that solubilization of the carrier provides efficient information about the state and location of the loops in the carrier. Therefore, we studied the effect of solubilization in Triton X-100 on bovine heart mitochondrial AAC. It has been thought that AAC in Triton-shells is functionally active, undergoing interconversion between m- and c-conformations (*12, 13*). However, it is not well studied whether the protein is completely intact or not.

This study shows that EMA, which has similar structural features to those of ADP/ATP (*14*), quickly and selectively labels Cys^{159} in the m-state carrier but not in the c-state carrier in Triton-shells, as observed with the membrane-bound carrier. This suggests that solubilization does not affect the affinity of the recognition site for ADP/ATP. Hence, the M2 loop could be located deep in the transmembrane region of the carrier inaccessible to detergent. In contrast to the stable conformation of the M2 loop in the solubilized carrier, a significant change was observed with the M1 loop. When the conformation of the carrier in Triton-shells was fixed in the m-state with BKA, an intramolecular disulfide bridge was formed between Cys^{56} in the M1 loop and Cys^{256} in the M3 loop. As the intermolecular disulfide bridge between two Cys^{56} residues is formed specifically with the membrane-bound carrier, intramolecular disulfide bridge formation characterizes the change in the state of AAC upon solubilization with Triton X-100. It is noteworthy that no disulfide bridge is formed in the solubilized c-state carrier. These results suggest that the M1 and M3 loops in the m-state carrier change their locations upon treatment with Triton X-100 in such a way that the opportunity for Cys^{56} to gain access for Cys^{256} is increased, in contrast to the stable conformation in the c-state carrier. As a result, intramolecular cross-linking of Cys^{56} with Cys^{256} takes place. The change in the location of the M3 loops is supported by the finding that Lys^{262} in the M3 loop of the carrier becomes susceptible to the lysine modifier pyridoxal 5-phosphate (PLP) upon solubilization of mitochondria with Triton X-100 (*15*).

It has been shown that the M1 loop of the membrane-bound carrier is cleaved first at the Lys^{42}-Gln^{43} bond and then at the Lys^{48}-Gln^{49} bond of the peptide fragment, suggesting that the segment containing the first site protrudes from the membrane, whereas that containing the second site becomes exposed due to an increase in its motional freedom after the first cleavage. Therefore, it could be that the segment containing Lys^{42} is completely exposed, and that the segment containing Lys^{48} is exposed and located in a position not readily accessible to lysylendopeptidase. These results are consistent with the fact that Lys^{42} and Lys^{48} in the m-state carrier are labeled with PLP from the matrix side (*15*).

Interestingly, upon solubilization in Triton X-100, proteolysis of the M1 loop took place almost simultaneously at both the Lys^{42}-Gln^{43} and Lys^{48}-Gln^{49} bonds, suggesting that the nonionic detergent causes the exposure of a segment containing the second cleavage site. Recently, we reported that the M1 loop fluctuates in a range centered at about 12 Å in the mitochondrial membrane (*6*). Upon solubilization, the M1 loop could acquire more motional freedom. The free fluctuation of the M1 loop by solubilization in Triton X-100 should be unfavorable for the formation of an inter-loop disulfide bridge, and should significantly increase the opportunity for Cys^{56} to come close to Cys^{256} in the same carrier molecule, but not to Cys^{159}. Therefore, the M1 loop should be located close to the M3 loop in the membrane, but not close to the M2 loop.

From the reactivities of the SH-reagents NEM and EMA

with cysteine residues of AAC, we previously thought that the M2 and M3 loops exist within the membrane region (*3*). However, the present results suggest that the M3 loop protrudes to some extent into the matrix space. Hence, it is possible that the M1 loop, which is exposed to the matrix side and fluctuating, changes conformation easily, and that the M3 loop, which is located near the surface of the membrane, becomes exposed to the matrix space under certain conditions. Access of the transport substrates ADP/ATP from the matrix side may cause greater fluctuation of the M1 loop and exposure of the M3 loop in the m-state carrier. This may then induce an interaction between these two loops, leading to the large translocation of the M1 loop required for transport activity (*5, 7*). Studies on the interaction of the M1 loop with the M3 loop will be important for understanding the transport mechanism of AAC.

REFERENCES

1. Klingenberg, M. (1993) Dialectics in carrier research: the ADP/ATP carrier and the uncoupling protein. *J. Bioenerg. Biomembr.* **25**, 447–457
2. Brandolin, G., Le Saux, A., Trezeguet, V., Lauquin, G.J.M., and Vignais, P.V. (1993) Chemical, immunological, enzymatic, and genetic approaches to studying the arrangement of the peptide chain of the ADP/ATP carrier in the mitochondrial membrane. *J. Bioenerg. Biomembr.* **25**, 459–472
3. Majima, E., Koike, H., Hong, Y.-M., Shinohara, Y., and Terada, H. (1993) Characterization of cysteine residues of mitochondrial ADP/ATP carrier with the SH-reagents eosin 5-maleimide and N-ethylmaleimide. *J. Biol. Chem.* **268**, 22181–22187
4. Majima, E., Shinohara, Y., Yamaguchi, N., Hong, Y.-M., and Terada, H. (1994) Importance of loops of mitochondrial ADP/ATP carrier for its transport activity deduced from reactivities of its cysteine residues with the sulfhydryl reagent eosin-5-maleimide. *Biochemistry* **33**, 9530–9536
5. Majima, E., Ikawa, K., Takeda, M., Hashimoto, M., Shinohara, Y., and Terada, H. (1995) Translocation of loops regulates transport activity of mitochondrial ADP/ATP carrier deduced from formation of a specific intermolecular disulfide bridge catalyzed by copper-o-phenanthroline. *J. Biol. Chem.* **270**, 29548–29554
6. Hashimoto, M., Majima, E., Goto, S., Shinohara, Y., and Terada, H. (1999) Fluctuation of the first loop facing the matrix of the mitochondrial ADP/ATP carrier deduced from intermolecular cross-linking of Cys56 residues by bifunctional dimaleimides. *Biochemistry* **38**, 1050–1056
7. Terada, H. and Majima, E. (1997) Important role of loops in the transport activity of the mitochondrial ADP/ATP carrier. *Progr. Colloid Polym. Sci.* **106**, 192–197
8. Beyer, K. and Nuscher, B. (1996) Specific cardiolipin binding interferes with labeling of sulfhydryl residues in the adenosine diphosphate/adenosine triphosphate carrier protein from beef heart mitochondria. *Biochemistry* **35**, 15784–15790
9. Krämer, R. (1986) Reconstitution of ADP/ATP translocase in phospholipid vesicles in *Methods in Enzymology* (Fleischer, S. and Fleischer, B., eds.) Vol. 125, pp. 610–618, Academic Press, New York
10. Laemmli, U.K. (1970) Cleavage of structural proteins during the assembly of the head of bacteriophage T4. *Nature* **227**, 680–685
11. Marty, I., Brandolin, G., Gagnon, J., Brasseur, R., and Vignais, P.V. (1992) Topography of the membrane-bound ADP/ATP carrier assessed by enzymatic proteolysis. *Biochemistry* **31**, 4058–4065
12. Block, M.R. and Vignais P.V. (1986) Dependence of the conformational state of the isolated adenine nucleotide carrier protein on the detergent used for solubilization. *Biochemistry* **25**, 374–379
13. Hoffmann, B., Stockle, A., Schlame, M., Beyer, K., and Klingenberg, M. (1994) The reconstituted ADP/ATP carrier activity has an absolute requirement for cardiolipin as shown in cysteine mutants. *J. Biol. Chem.* **269**, 1940–1944
14. Majima, E., Yamaguchi, N., Chuman, H., Shinohara, Y., Ishida, M., Goto, S., and Terada, H. (1998) Binding of the fluorescein derivative eosin Y to the mitochondrial ADP/ATP carrier: characterization of the adenine nucleotide binding site. *Biochemistry* **37**, 424–432
15. Bogner, W., Aquila, H., and Klingenberg, M. (1986) The transmembrane arrangement of the ADP/ATP carrier as elucidated by the lysine reagent pyridoxal 5-phosphate. *Eur. J. Biochem.* **161**, 611–620